Elastic knots

B. Audoly,* N. Clauvelin, and S. Neukirch
Institut Jean le Rond d'Alembert,
UMR 7190: CNRS & Université Pierre et Marie Curie, Paris, France
(Dated: September 4, 2007)

We study the mechanical response of elastic rods bent into open knots, focusing on the case of trefoil and cinquefoil topologies. The limit of a weak applied tensile force is studied both analytically and experimentally: the Kirchhoff equations with self-contact are solved by means of matched asymptotic expansions; predictions on both the geometrical and mechanical properties of the elastic equilibrium are compared to experiments. The extension of the theory to tight knots is discussed.

PACS numbers: 46.25.-y, 46.70.Hg,

Knots have long been considered mainly from a mathematical perspective but this topic has today spread to different areas in science. Fishermen and sailors know that tying a knot on a rope severely reduces its tensile strength [1]. More recently knots have been tied on biological molecules [2], micrometric silica wires [3], or lipid-bilayer nanotubes [4] and their properties were compared to unknotted configurations. Sufficiently long polymers often adopt knotted configurations spontaneously [5]. A recent survey identified 273 knotted proteins [6, 7], although the biological function of these knots remains unclear. Knots are also found in DNA plasmids and the electrophoretic mobility of a knotted DNA molecule is related to its topological properties [8].

To date, the tightening of knots has been studied based on molecular dynamics or *ab initio* methods [9], methods from statistical physics [10], purely geometrical models [11], or perfectly flexible rod models [12]. In this Letter, we investigate the mechanical response of knots based on the theory of elasticity. The equilibrium con-

FIG. 1: Geometry of an open trefoil knot (3_1) under tension. Inset: open cinquefoil knot (5_1).

figurations of open trefoil (3_1) and cinquefoil (5_1) knots are analyzed, see Fig. 1; other knot types can be handled similarly.

Consider an infinitely long elastic rod with circular cross section of radius h, flexural modulus EI, bent into an open knot. The rod is held by a tensile force T applied at both ends and contacts itself in a braided region. In the $h = 0$ case, the solution consists of two straight, half-infinite tails connected by one circular loop with radius

R. Minimizing the sum of bending energy $\left[(2\pi R)\frac{1}{2}\frac{EI}{R^2}\right]$ and potential energy $2\pi R T$ accounting for the applied tension yields [2]:

$$T = EI/(2R^2). \tag{1}$$

Here, we determine the shape and mechanical response of knots for small but nonzero h. The entanglement, which takes place at a point for $h = 0$, remains localized for small h [13]. We solve the Kirchhoff equations for inextensible, unshearable rods with circular cross section:

$$\mathbf{r}' = \mathbf{t}, \quad \mathbf{t}' = (\mathbf{M}/EI) \times \mathbf{t} \tag{2a}$$

$$\mathbf{M}' + \mathbf{t} \times \mathbf{N} = \mathbf{0}, \quad \mathbf{N}' + \mathbf{p} = \mathbf{0}. \tag{2b}$$

where s is the arc length, $\mathbf{t}(s)$ is the unit tangent to the 3D centerline $\mathbf{r}(s)$, $\mathbf{M}(s)$ the internal moment, $\mathbf{N}(s)$ the internal force, and $\mathbf{p}(s)$ the contact pressure (homogenous to a force per unit length). Primes denote derivatives with respect to s. The main difficulty lies in the non-penetration condition:

$$|\mathbf{r}(s_1) - \mathbf{r}(s_2)| \geq 2h \tag{3}$$

that must hold for all s_1 and s_2 (with $|s_1 - s_2|/h$ large enough to exclude neighboring points from the test). In such self-contact problems, the contact set and contact pressure $\mathbf{p}(s)$ have to be determined in a self-consistent way. Another difficulty is that the topology of contact set is not known beforehand [14]. Problems involving isolated points of contact [15], or contact sets comprising straight lines [16], have been treated. An axial tension is applied at both ends but the latter can freely twist; as a result, the moment of twist $\mathbf{M} \cdot \mathbf{t}$, which is uniform along the rod, is zero everywhere.

We build a solution of Kirchhoff equations (2) for a knotted configuration in the small h limit. The rod is divided into three regions: two outer regions (tails and loop) and an inner region (braid) where contact takes place. We introduce the small parameter $\epsilon = (h/R)^{1/2}$ and perform a matched asymptotic expansion of solutions to (2) in the different regions. We first derive a
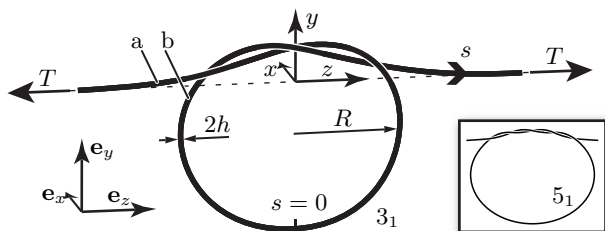
scaling law for the length ℓ of the braid, assuming ℓ is an intermediate quantity, $h \ll \ell \ll R$. In the braid, of length ℓ, transverse displacements are of order h: the centerline has a slope of order h/ℓ with respect to the z axis. Points in the loop at a distance of order ℓ from the axis of symmetry y have a slope $\sim \ell/R$. Equating these two slopes requires ℓ to be of order $\sqrt{h\,R}$.

The rod configuration in the tails is found, to first order in ϵ, by solving equations (2) linearized near the straight configuration ($\mathbf{t} = \mathbf{e}_z$, $\mathbf{M} = 0$ and $\mathbf{N} = T\,\mathbf{e}_z$), where $\mathbf{e}_{x,y,z}$ are unit vectors defined in Fig. 1. The first order correction for the tails is found to have an exponential profile, proportional to $e^{-|z|\sqrt{T/EI}}$. Similarly, the loop part is solved to first order by linearizing equations (2) near a circular configuration $\mathbf{t} = \sin(s/R)\,\mathbf{e}_y - \cos(s/R)\,\mathbf{e}_z$, $\mathbf{M} = (EI/R)\mathbf{e}_x$ and $\mathbf{N} = \mathbf{0}$, where $-\pi R < s < \pi R$. The perturbed loop configuration is found to remain planar, although in a plane that is slightly tilted about the y axis. The details of the calculations are omitted.

Let us proceed to the inner solution. The braid is the crucial region where the external tensile load T in the tails is transformed, with the help of contact forces, into the internal bending moment EI/R in the loop. According to the previous scalings, the slope in the braid is small, of order ϵ. Geometric nonlinearities can then be neglected and the leading order of system (2) for strand 'a', with centerline $\mathbf{r}_{\mathrm{a}} = (x_{\mathrm{a}}, y_{\mathrm{a}}, z_{\mathrm{a}})$, reads: $EI x_{\mathrm{a}}'''' = p_{\mathrm{a}}^x$, $EI y_{\mathrm{a}}'''' = p_{\mathrm{a}}^y$, $z_{\mathrm{a}}' = 1$ where $p_{\mathrm{a}}^x = |\mathbf{p}|\,(x_{\mathrm{b}} - x_{\mathrm{a}})/(2h)$ and $p_{\mathrm{a}}^y = |\mathbf{p}|\,(y_{\mathrm{b}} - y_{\mathrm{a}})/(2h)$ are the components of the contact force, assuming that there is no friction. The equations for the other strand 'b' are similar, with $p_{\mathrm{b}}^x = -p_{\mathrm{a}}^x$ and $p_{\mathrm{b}}^y = -p_{\mathrm{a}}^y$ by the action-reaction principle. We take advantage of the linearity of these equations and separate the inner problem into an average and a difference problem. To this end, we introduce the new variables $\langle \mathbf{r}(s) \rangle = (\mathbf{r}_{\mathrm{a}}(s) + \mathbf{r}_{\mathrm{b}}(s))/2$ and $\bar{\mathbf{r}} = (\mathbf{r}_{\mathrm{b}}(s) - \mathbf{r}_{\mathrm{a}}(s))/2$.

The average problem gives the position of the curve lying halfway in between the two strands. It obeys the Kirchhoff linearized equations: $EI\langle x \rangle'''' = 0$, $EI\langle y \rangle'''' = 0$, with the asymptotic conditions $\langle x \rangle'' = 1/(2R)$ at both ends to allow matching with the loop. Note that the contact forces cancel out in the average problem. As a result, it has an obvious solution, namely an arc of circle with radius $2R$, up to a rigid-body rotation and translation.

The difference problem tells how the two strands contact and wind around each other. The components of $\bar{\mathbf{r}}$ satisfy the Kirchhoff linearized equations: $EI\,\bar{x}'''' = |\mathbf{p}|\,\bar{x}/h$, $EI\,\bar{y}'''' = |\mathbf{p}|\,\bar{y}/h$. Based on the previous scaling analysis, we introduce the rescaled quantities:

$$u = \frac{x_{\mathrm{b}} - x_{\mathrm{a}}}{2\,h}, \quad v = \frac{y_{\mathrm{b}} - y_{\mathrm{a}}}{2\,h}, \quad w = \frac{z}{(2\,h\,R)^{1/2}}. \quad (4)$$

Since the tangent deviates only slightly from $\mathbf{e}_z$, the arc length $s \simeq z$, or w in rescaled coordinates, can be used
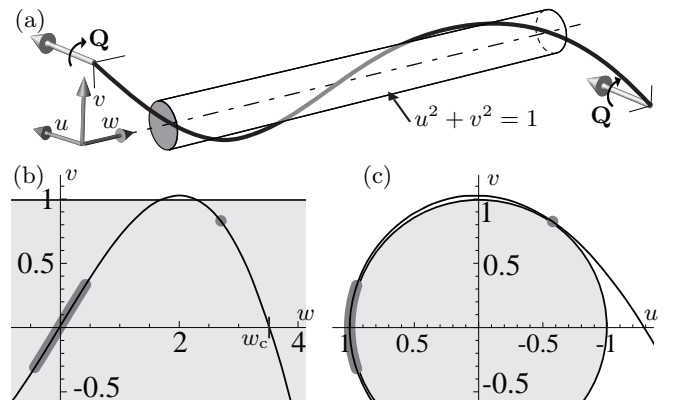

FIG. 2: Difference problem for the braid region. (a) Geometry. (b) Visualization of the solution for a trefoil knot, projected in the (v, w) plane, and (c) in the plane (u, v) perpendicular to the axis of the cylinder. Only one half of the symmetric solution is shown. Contact is denoted with thick curves and points.

to parameterize the deflection given by u and v. The unknowns of the difference problem are the functions $u(w)$ and $v(w)$. As mentioned earlier, the contact set is not known beforehand in this kind of problems. However, the non-penetration condition (3) takes a simple form:

$$u^2(w) + v^2(w) \geq 1 \quad \text{for all } w. \quad (5)$$

The self-contact problem then reduces to finding the configuration of an effective 'difference' Kirchhoff rod in (partial) contact with a fixed external object, namely a cylinder, as shown in Fig. 2a. Making use of the variational structure underlying the Kirchhoff equations, we seek the solutions $u(w)$ and $v(w)$ as minimizers of the following energy:

$$\mathcal{E}_\Delta = \int_{-W}^{+W} \frac{u''^2(w) + v''^2(w)}{2}\,dw + v'(W) + v'(-W), \quad (6)$$

subjected to the non-penetration constraint (5), and to the constraint that the 'difference' rod makes a prescribed number of turns around the cylinder: one and a half turn for trefoil knots and two and a half turns for cinquefoil knots. The first term in this energy is the bending energy, proportional to the curvature squared. The last two terms are the work done by the moments $\mathbf{Q}$ along $\mathbf{e}_u$ coming from the loop region, as shown in Fig. 2a. The length $2W$ of the domain is an arbitrary, large number: the minimizers do not depend on W as long as W is beyond the endpoint of the contact region.

We solve the variational problem (5)–(6) with standard numerical routines for constrained minimization. Note that there is no numerical parameter left in the formulation. The solution for a trefoil knot is shown in Fig. 2b and c. The topology of the contact is non trivial: around the center ($w = 0$) of the braid, there is an extended
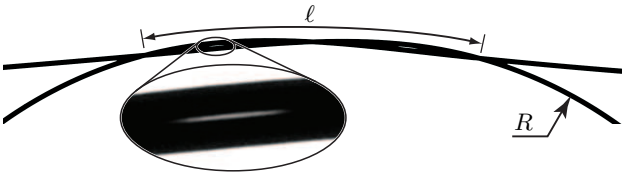
FIG. 3: Photograph and close-up of an experimental braid, with $\epsilon \approx .074$. The two symmetric openings are predicted by the theory.
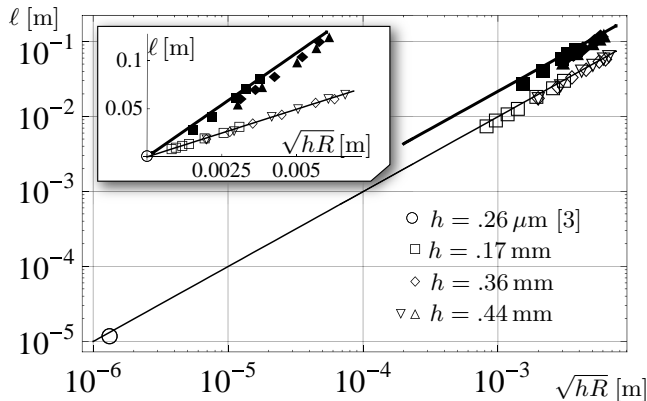

FIG. 4: Braid length ℓ versus intermediate length $(h\,R)^{1/2}$ in log-log plot. In inset, the same data is shown in linear plot. Open symbols and thin line are for trefoil knots. Filled symbols and thick line are for cinquefoil knots. All rods are Nitinol wires, except for the single circular data-point, computed from data from Ref. [3]. The lines are the theoretical prediction (7), with no adjustable parameter.

region $|w| \leq 0.348$ with continuous contact. Further away from the center, the 'difference' rod lifts off from the cylinder to reach, at $w = \pm 1.823$, a maximum gap of $\sqrt{u^2 + v^2} - 1 = 0.021$ in rescaled units (implying a gap of $0.021 \times (2h) = 4.3\% \times h$ in physical units). This opening ends up with an isolated contact at $w = \pm 2.681$ where the strands eventually separate for good. The two symmetric gaps (for positive and negative w) can be observed experimentally, as shown in Fig. 3. The contact topology is the same in the case of cinquefoil knots (5_1), the central region with continuous contact being wider. The solution $v(w)$ to the difference problem vanishes at $w = w_c$, see Fig. 2b. This corresponds to an apparent crossing of the two strands, as viewed from the side (along the direction $\mathbf{e}_u \approx \mathbf{e}_x$). We use this crossings to define the length ℓ of the braid, see Fig. 3. In rescaled units, this length is $2\,w_c$ that is, in physical units:

$$\ell = 2\,w_c\,\sqrt{2\,h\,R}, \qquad (7)$$

where $w_c = 3.506$ for trefoil knots, while $w_c = 7.640$ for cinquefoil knots. This theoretical prediction is compared with experiments for both kinds of knots, and a good quantitative agreement is found, see Fig. 4. In exper-

iments, we used naturally straight, super-elastic wires made of Nitinol, an alloy of nickel and titanium, with various diameters in the millimetric range and length $L \approx 2$ m; we checked that the rods returned to their natural straight configuration after the experiments (no plastic deformation). Note that in fig. 4, we also included a data-point that we measured from the image of a knotted silica wire with radius 260 nm obtained by scanning electron microscopy in Ref. [3, Fig. 3a].

It is possible to account for weak friction in the braid using the present framework. The total contact force, from one strand to the other, is $P = \int_{-\ell/2}^{\ell/2} |\mathbf{p}(s)|\,\mathrm{d}s = \sigma\,EI\,R^{-3/2}\,h^{-1/2}$, where σ is a numerical constant computed from the inner solution, $\sigma = .492$ for trefoil knots, and $\mathbf{p}(s)$ is the radial contact force pointing outwards. When the strands are sliding along each other in the braid, a friction force $\pm\mu\,P$ builds up, where μ is the dynamic Coulomb friction of the rod onto itself. As a result, the relation (1) between the applied tension and the loop radius has to be modified as follows:

$$\frac{T\,h^2}{EI} = \frac{\epsilon^4}{2} \pm \mu\,\sigma\,\epsilon^3. \qquad (8)$$

The first term is the elastic contribution, as in equation (1), while the second term accounts for friction forces, with a sign that depends on whether the knot is being tightened (+) or loosened (−). The experimental response curve for a trefoil knot made with a coated Nitinol rod of diameter .89 mm is shown in Fig. 5, and
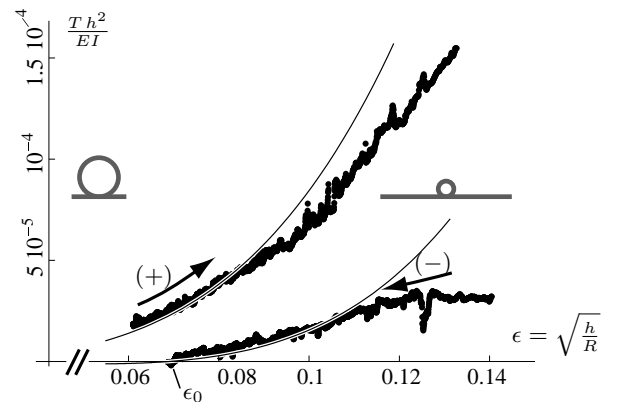

FIG. 5: Traction-displacement curve for a Nitinol wire with a trefoil knot. The knot is first tightened (upper curve) and then loosened (lower curve) until it becomes locked by friction, for a value $\epsilon = \epsilon_0$. The curves are the theoretical prediction (8), with the Coulomb friction coefficient adjusted to $\mu = .07$ from equation (9). There is no other adjustable parameter in the plot. The agreement between theory and experiments is good as soon as $\epsilon \lesssim 0.1$.

compared to the predictions of equation (8). It was obtained by attaching one end to a force probe, while the other end was first pulled, and then relaxed, at a velocity of order 1 mm/s. We were careful to keep the tails

long enough (typically 50 cm long) to avoid any end effect coming from the clamped ends of the rod. The parameter R, required to plot the curves as a function of $\epsilon = \sqrt{h/R}$, is determined from the shortening ΔL of the rod with respect to its unknotted configuration, divided by 2π. Stick-slip takes place, as revealed by the spikes in the experimental curves, but it was minimized by laying the knot horizontally on a large block of material with low friction (Teflon). Negative values of the traction T are not accessible in this experiment as the tails buckle: we stopped the experiments when the tension reaches $T = 0$. Then, the knot is locked by friction. From equation (8) the corresponding values of R_0 and $\epsilon_0 = \sqrt{h/R_0}$ satisfy $\epsilon_0 = 2\,\mu\,\sigma$ and so

$$\mu = \frac{1}{2\sigma}\epsilon_0 = 1.02\,\sqrt{h/R_0}, \qquad (9)$$

using the numerical value of σ relevant for a trefoil knot. With the help of this formula, one can measure the self-friction coefficient μ from a simple experiment, by tightening the knotted rod, releasing its ends, letting the loop grow spontaneously and measuring the final radius R_0. Using this method with the data shown in Fig. 5, we find $\mu = 0.07$. This is consistent with a direct (but inaccurate) measurement of the longitudinal force between two pieces of the rod sliding along each other (taking care to minimize stick-slip as much as possible), which gives $\mu \approx .1$.

We have obtained an analytical solution for the equilibrium configurations of open elastic knots, which is exact in the limit of loose knots, that is for small ϵ. The theory shows good quantitative agreement with experiments performed on elastic rods, concerning both the geometry of the solution and the traction curves. A natural extension of the work presented here is the study of the behavior of tight knots, that is when ϵ is no longer small, $\epsilon = \mathcal{O}(1)$. This question has been addressed from a purely geometrical perspective through the problem of ideal knots [17, 18]. In such geometrical models, tight open knots typically exhibit a maximum of curvature in the region where the tails enter the entangled region [11]. Simulations based on the elastic model are in contradiction with this result. In Fig. 6, we show preliminary results concerning the solutions of equations (2) and (3) for a tight elastic knot with $\epsilon = \sqrt{\frac{h}{\Delta L/(2\pi)}} = .52$, and compare with the geometrical model of Ref. [11] for which $\epsilon = .56$. The large, oscillatory curvature obtained in [11] at the exit of the knot seems to point to the fact that the geometrical problem is ill-posed in the matching region between the perfectly straight tails and the knot; these oscillations are regularized by elasticity. In the geometric case, the point of maximum curvature is at the exit of the knot ($s/h \simeq \pm 10$); in the elastic case, this maximum lies well inside the knot (points a and c in the figure, for $s/h \simeq \pm 6$). This leaves open the question of where a tight know will actually break. By pushing further the
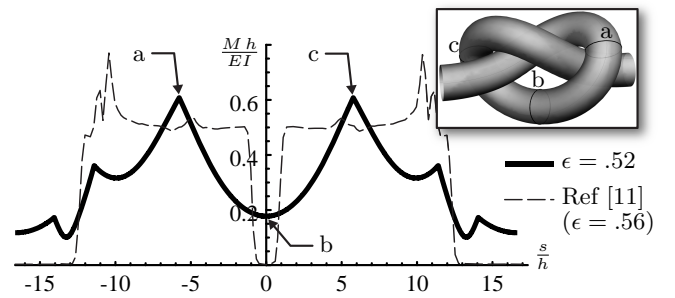

FIG. 6: Curvature of a tight elastic trefoil knot ($\epsilon = 0.52$, bold curve), and comparison with the geometrical calculation of a tight trefoil knot in Ref. [11] (dotted).

present mechanical analysis, one can derive the distributions of strains in the material and attempt to answer this question.

It is a pleasure to thank B. Roman and J. Bico from the Laboratoire PMMH (ESPCI) for their help in setting up the experiments, and J. Maddocks for providing some of the Nitinol rods.

* URL: http://www.lmm.jussieu.fr/~audoly/
[1] A. Stasiak, A. Dobay, J. Dubochet, G. Dietler, H. E. Gaub, H. Clausen-Schaumann, M. Beyer, M. Rief, and M. Grandbois, Science **286**, 11a (1999).
[2] Y. Arai, R. Yasuda, K.-I. Akashi, Y. Harada, H. Miyata, K. Kinosita, and H. Itoh, Nature **399**, 446 (1999).
[3] L. Tong, R. R. Gattass, J. B. Ashcom, S. He, J. Lou, M. Shen, I. Maxwell, and E. Mazur, Nature **426**, 816 (2003).
[4] T. Lobovkina, P. Dommersnes, J.-F. Joanny, P. Bassereau, M. Karlsson, and O. Orwar, PNAS **101**, 7949 (2004).
[5] D. W. Sumners and S. G. Whittington, Journal of Physics A: Mathematical and General **21**, 1689 (1988).
[6] M. L. Mansfield, Nature Structural and Molecular Biology **1**, 213 (1994).
[7] P. Virnau, L. A. Mirny, and M. Kardar, PLoS Computational Biology **2**, 1074 (2006).
[8] A. Stasiak, V. Katritch, J. Bednar, D. Michoud, and J. Dubochet, Nature **384**, 122 (1996).
[9] A. M. Saitta, P. D. Soper, E. Wasserman, and M. L. Klein, Nature **399**, 46 (1999).
[10] O. Farago, Y. Kantor, and M. Kardar, Europhysics Letters (EPL) **60**, 53 (2002).
[11] P. Pieranski, S. Przybyl, and A. Stasiak, The European Physical Journal E - Soft Matter **6**, 123 (2001).
[12] J. H. Maddocks and J. B. Keller, SIAM Journal on Applied Mathematics **47**, 1185 (1987).
[13] R. Gallotti and O. Pierre-Louis, Physical Review E (Statistical, Nonlinear, and Soft Matter Physics) **75**, 031801 (2007).
[14] H. von der Mosel, Annales de l'I. H. P., section C **16**, 137 (1999).
[15] G. H. M. van der Heijden, S. Neukirch, V. G. A. Goss,

and J. M. T. Thompson, International Journal of Mechanical Sciences **45**, 161 (2003).

[16] B. Coleman and D. Swigon, Journal of Elasticity **60**, 173 (2000).

[17] A. Stasiak, V. Katritch, and L. H. Kauffman, eds., *Ideal Knots* (World Scientific, Singapore, 1998).

[18] J. Baranska, P. Pieranski, S. Przybyl, and E. J. Rawdon, Phys. Rev. E **70**, 051810 (2004).